Document No.: TRPCS- ATBD-036

Time-Resolved Observations of Precipitation structure and storm Intensity with a Constellation of Smallsats

Atmospheric Vertical Temperature and Moisture Profiles

Algorithm Theoretical Basis Document

27 September 2023

Revision 1.5

National Aeronautics and Space Administration
Goddard Earth Science Data Information and Services Center (GES DISC)

Prepared by: Tom Greenwald & Ralf Bennartz Date: __________
UW-Madison SSEC & Vanderbilt Univ.

Approved by:
____ Date: __________
William J. Blackwell
TROPICS Principal Investigator
MIT Lincoln Laboratory

Approved by: ____ Date: __________
Scott Braun
TROPICS Project Scientist
NASA Goddard Space Flight Center

Approved by: ____ Date: __________
R. Vincent Leslie
TROPICS Project Manager
MIT Lincoln Laboratory

LINCOLN LABORATORY
MASSACHUSETTS INSTITUTE OF TECHNOLOGY

Revision History

Version	*Description*	*Date*	*Initiator*
0.1	Initial Draft	07/26/2017	Vince Leslie
0.2	Expanded draft	08/04/2017	Tom Greenwald
0.3	Added ISRR description	09/13/2017	Tom Greenwald
1.0	Results based on latest instrument design	11/27/2017	Tom Greenwald
1.1	Improved moisture profile performance	04/23/2018	Tom Greenwald
1.2	Removed ISRR materials	04/01/2019	Vince Leslie
1.3	Added NOAA88 dataset results and averaging kernel analysis	11/01/2019	Tom Greenwald
1.4	Added discussion on CRTM polarization mixing angle and instrument SRF	06/11/2021	Tom Greenwald
1.5	Added GEOS-5 NWP ancillary data discussion & polarization update	09/27/2023	Tom Greenwald & Vince Leslie

Contents

1 Scope

This Algorithm Theoretical Basis Document (ATBD) describes the theoretical background of the TROPICS Atmospheric Vertical Temperature and Moisture Profile (AVTP/AVMP) retrieval algorithms. It also includes TROPICS payload characteristics and the algorithm's ancillary data (i.e., data coming from sources other than the TROPICS Space Vehicle). Details of the AVTP and AVMP, data product format can be found in the TROPICS Data User's Guide. This ATBD will also contain the pre-launch testing completed to verify the algorithm. The TROPICS Data User's Guide will contain the post-launch validation.

2 System Overview

The Time-Resolved Observations of Precipitation structure and storm Intensity with a Constellation of Smallsats (TROPICS) mission [1] will provide rapid-refresh microwave measurements over the tropics that can be used to observe the thermodynamics of the troposphere and precipitation structure for storm systems at the mesoscale and synoptic scale over the entire storm lifecycle. TROPICS comprises a constellation of six CubeSats in three low-Earth orbital planes. Each CubeSat will host a high-performance radiometer scanning across the satellite track at 30 RPM to provide temperature profiles using seven channels near the 118.75 GHz oxygen absorption line, water vapor profiles using 3 channels near the 183 GHz water vapor absorption line, imagery in a single channel near 90 GHz for precipitation measurements, and a single channel at 206 GHz for cloud ice measurements. This observing system offers an unprecedented combination of horizontal and temporal resolution to measure environmental and inner-core conditions for tropical cyclones (TCs) on a nearly global scale and is a profound leap forward in the temporal resolution of several key parameters needed for detailed study of high-impact meteorological events (e.g., Tropical Cyclones). TROPICS will demonstrate that a constellation approach to earth Science can provide improved resolution, configurable coverage (tropics, near global, or global), flexibility, reliability, and launch access at extremely cost effective, thereby serving as a model for future missions.

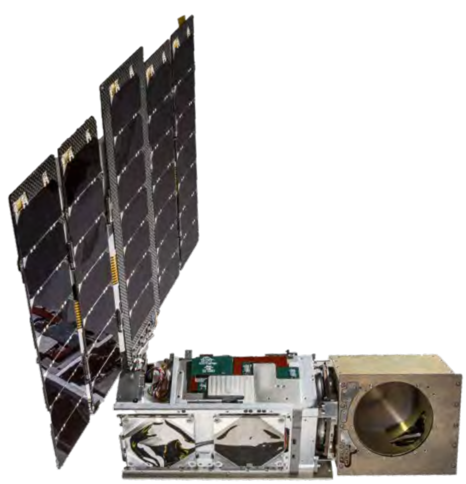

Figure 1 Photo of TROPICS Space Vehicle

3 Applicable TROPICS Documents

1. TROPICS Data Product User Guide: Publicly released document with information on payload and space vehicle characteristics, quality flags, and validation along with full data product format description.
2. TROPICS Radiometric Calibration ATBD (Level-1a and Level-1b data products)
3. TROPICS Unified Resolution Radiometric Product ATBD (Level-2a data product)
4. TROPICS Instantaneous Surface Rain Rate (ISRR) ATBD (Level-2b data product) using the Goddard NASA PRPS algorithm
5. TROPICS Tropical Cyclone Intensity ATBD (Level-2b data product consisting of Minimum Sea-Level Pressure and Maximum Sustained Wind Speed)

4 Payload Characteristics

This section presents the TROPICS payload characteristics. The payload is a total-power radiometer with channels at W, F, and G bands.

4.1 Receiver Architecture

Table 1 contains the spectral passbands, spatial beamwidth, and expected Noise Equivalent Delta Noise (NEdT) of the channels. TROPICS weighting functions can be found in the TROPICS Level-2b AVP ATBD. Each SV's NEDT can be found in Appendix A: Noise Equivalent Delta Noise. A complete list of individual beamwidths can be found in Appendix B: Antenna Pattern Beamwidths (Full-width Half Max.).

Table 1 TROPICS spectral and spatial Stats (Footprint from 550-km altitude)

Chan.	Center Freq. (GHz)	Band width (GHz)	RF Span (GHz)	Beamwidth (degrees) Down/Cross	Nadir Footprint Geometric Mean (km)
1	91.655 ± 1.4	1.000	89.756-90.756, 92.556-93.556	3.0/3.17	29.6
2	114.50	1.000	114.00-115.00	2.4/2.62	24.1
3	115.95	0.800	115.55-116.35	2.4/2.62	24.1
4	116.65	0.600	116.35-116.95	2.4/2.62	24.1
5	117.25	0.600	116.95-117.55	2.4/2.62	24.1
6	117.80	0.500	117.55-118.05	2.4/2.62	24.1

7	118.24	0.380	118.05-118.43	2.4/2.62	24.1
8	118.58	0.300	118.43-118.73	2.4/2.62	24.1
9	184.41	2.000	183.41-185.41	1.5/1.87	16.1
10	186.51	2.000	185.51-187.51	1.5/1.87	16.1
11	190.31	2.000	189.31-191.31	1.5/1.87	16.1
12	204.8	2.000	203.8-205.8	1.4/1.76	15.2

The receiver architecture consists of two separate receiver chains. A simplified payload block diagram is shown in Figure 2. The W- and F-band channels (i.e., Chan. 1 through 8) are implemented with a superheterodyne radiometer. The W-band channel is double sideband, and the F-band channels are single sideband. The W/F receiver has a local oscillator with a fundamental frequency of 30.552 GHz. The G-band channels are implemented with a direct-detect radiometer using single sidebands.

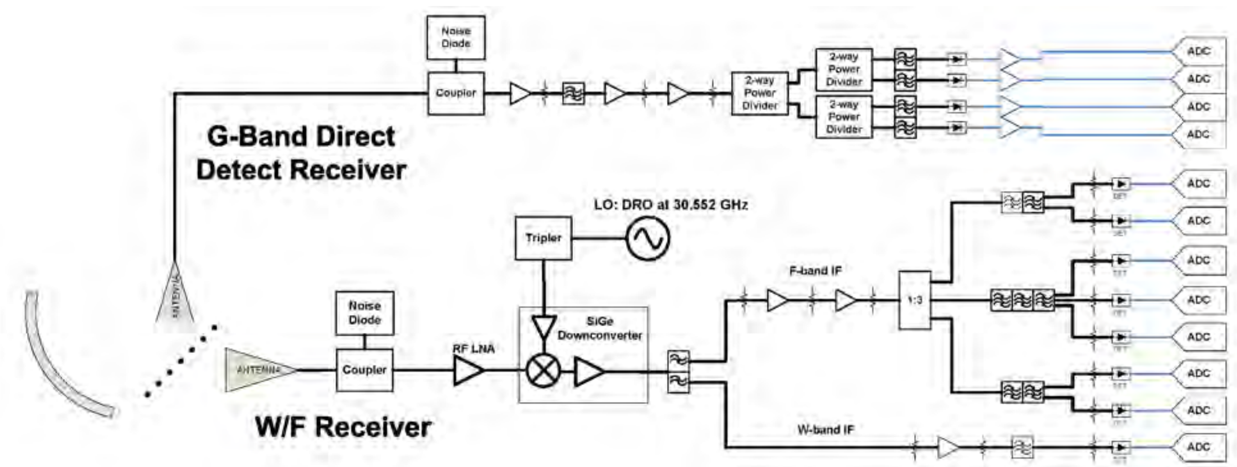

Figure 2 Simplified TROPICS payload block diagram

4.2 Spatial Response

Figure 2 also has a simple illustration of the antenna subsystem. Inside the payload is an offset parabolic reflector with separate feedhorns for the W/F-band receiver and the G-band receiver. The feedhorns illuminate the reflector through a wire gird polarizer, which allow the incoming radiation to be diplexed. More information on polarization is in Sect. 4.3. Figure 3 is an illustration of the TROPICS cross-track scan. The scan is implemented by spinning the entire payload "cube" in reference to the spacecraft bus. Similar to a conical scanner, TROPICS uses a motor and slipring to rotate the payload, but in a cross-track scan pattern on the surface. Table 2 contains the scan pattern details for the cross-track swath projected beneath the space vehicle. There are 81 spots or beam positions in the Earth View Sector. TROPICS scans during the integration period; therefore, the cross-track dimension will be larger than the down-track dimension. Due to the wire grid, the TROPICS footprints will have minimal offset on the ground, which is a tremendous advantage in post-processing. Sect. 1 has a table of the dimensions of each footprint separated out by band (W, F, G, and 205 GHz) and track. To compare the swath width to ATMS, Figure 4 plots the footprints of the spots on the Earth's surface, along with the ATMS footprints.

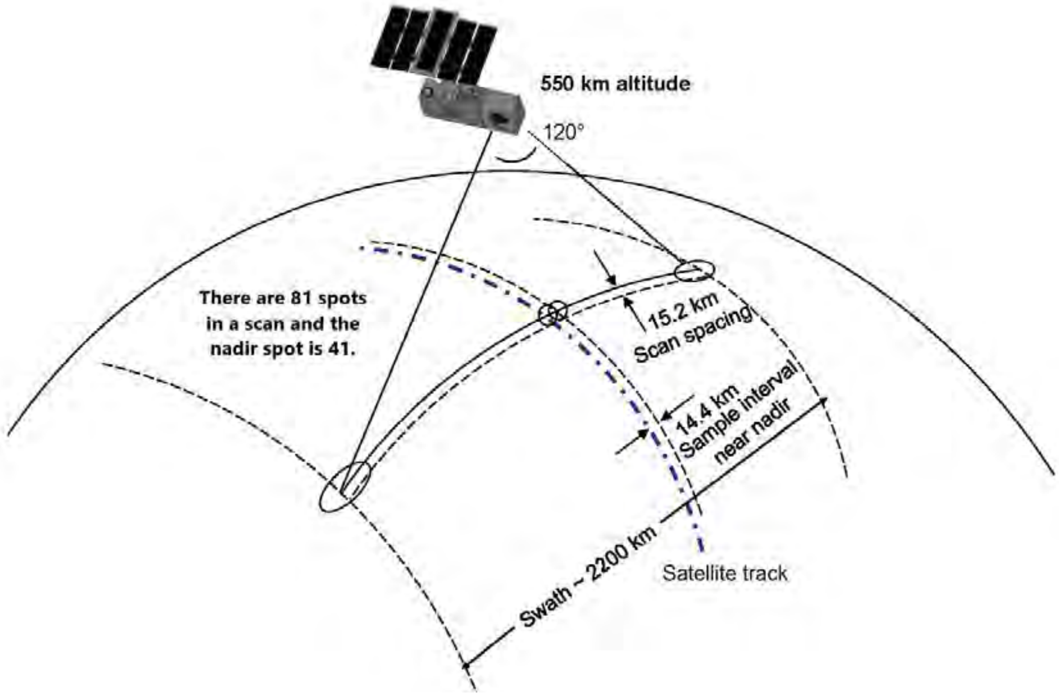

Figure 3 Illustration of the TROPICS cross-track scan pattern.

Table 2 TROPICS scan profile characteristics

Characteristic	Units	Value
Rotation Period	Seconds	2
Maximum Earth View Sector Angle	Degrees	± 60
Scan Type	N/A	Constant velocity (scanning during integration)
Integration time	Seconds	1/120
Number of Earth View Sector Measurements	N/A	81 per scan (one at nadir)

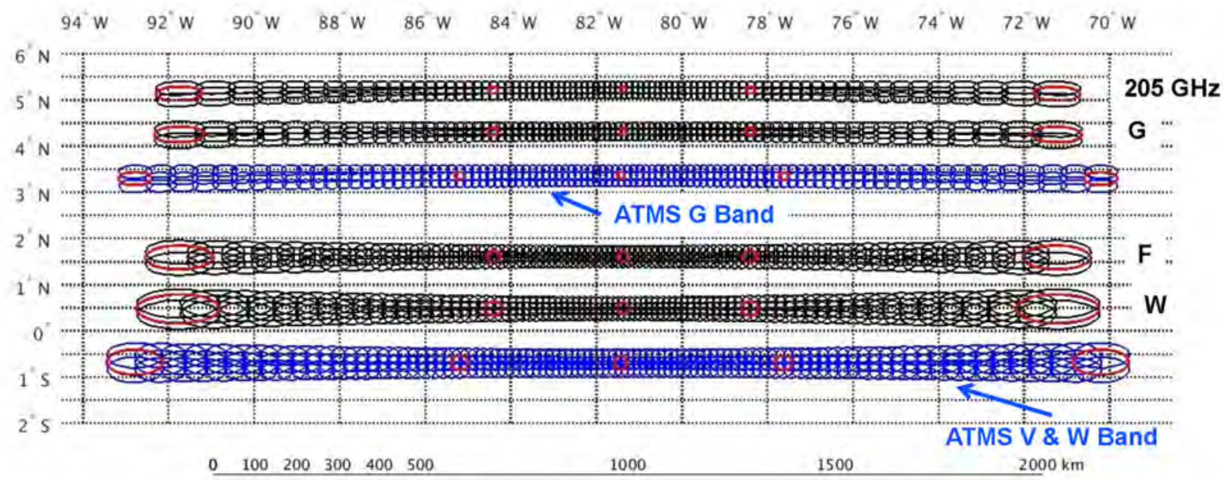

Figure 4 TROPICS swath comparison against ATMS. TROPICS' altitude for this rendering was 550 km.

4.3 Polarization

As previously mentioned, the TROPICS payload has a non-traditional polarization. Figure 5 illustrates the TROPICS polarization, which is a combination of the traditional conical scanner (i.e., fixed angle between reflector and feedhorn) and the cross-track scanner (i.e., scan angle to zenith angle conversion at the surface). As illustrated in the upper left-hand side, the polarization is fixed for the W band at 16 deg. and F band at 14 deg. (i.e., Phi, φ, in the figure, which is called the polarization angle), while the G-band will be -76 deg. per the angle φ defined in the figure. This makes the polarization largely the same as the upwelling horizontal and vertical polarization. This is true for all bands. The polarization will be measured pre-launch, but is expected to be close to the above values. The mixing equation is given in Equation 1. Phi, φ, is typically the scan angle in traditional cross-track radiometers, but the TROPICS feedhorn moves with the reflector (and the entire payload) and therefore remains constant while the entire payload rotates. In the

Equation 1 $$T_b = T_b^{hori} * cos^2(\varphi) + T_b^{vert} * sin^2(\varphi)$$

spaceborne radiative transfer equation (not shown), the polarized sources of radiation for the TROPICS instrument is the ocean surface, while the atmosphere and land are largely unpolarized.

Figure 6 is a simulation of the ocean emissivity versus instrument scan angle. The solid black and blue lines are the surface emissivity's vertical and horizontal components, respectively. The solid green in the mixed polarization where the polarization angle is 16 deg. (for W band) for the TROPICS receiver. For comparison, the typical cross-track "quasi" polarization, which has the same equation as Equation 1, but with Phi, i.e., the polarization angle, replaced with the changing scan angle.

Finally, Figure 7 shows an idealized simulated brightness temperature as a function of scan angle with the fixed 16/14/-76 deg. polarization angle for a tropical ocean surface. There is limb darkening or brightening due to the change in thickness of the atmosphere and surface emissivity. This simulation does not model antenna pattern sidelobes (i.e., it is a Gaussian beam).

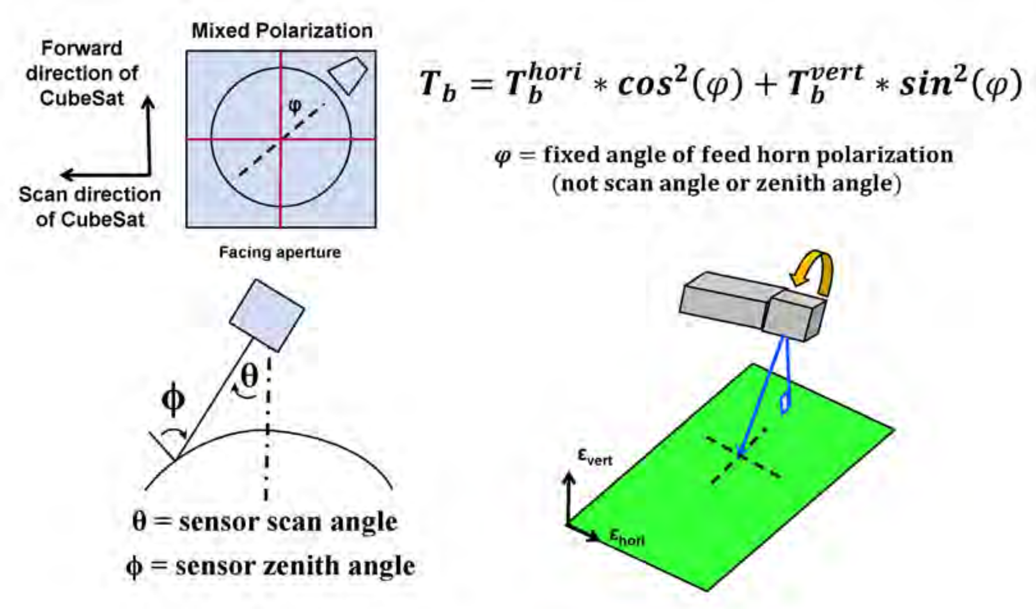

Figure 5 Illustration explaining the TROPICS polarization.

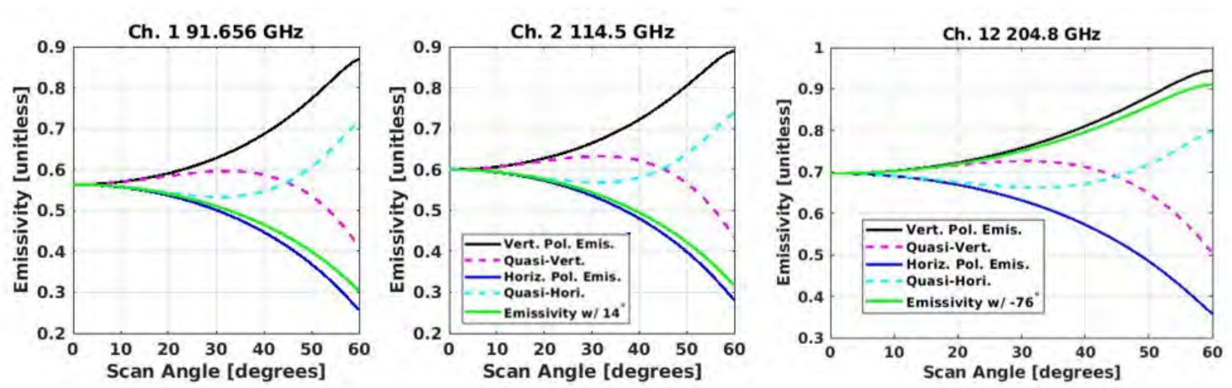

Figure 6 Simulated ocean surface emissivity (fastem v2)

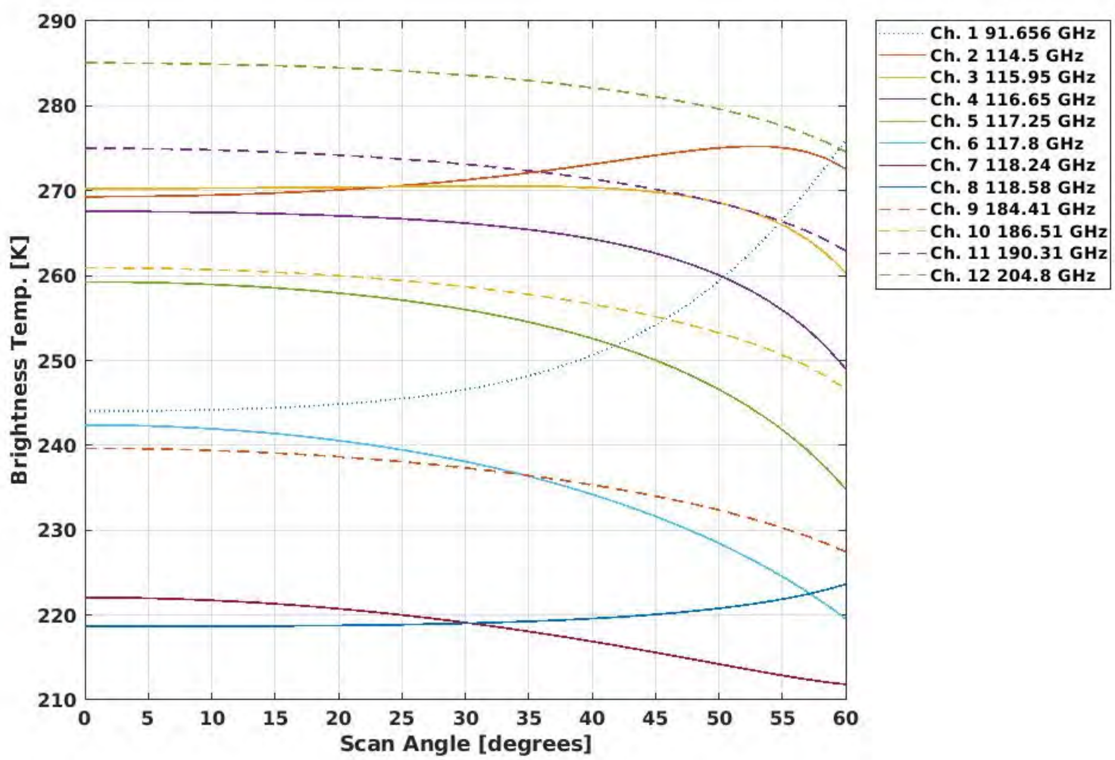

Figure 7 Simulated brightness temperature vs sensor scan angle from the tropical US Standard 1976 atmosphere and fastem version 2 ocean emissivity model. W/F-band at 16/14 deg. and G-band at -76 deg.

5 Data Products

A comprehensive data product description can be found in the TROPICS Data User's Guide. A high-level description of the data products is given in Table 3.

Table 3 TROPICS data product descriptions.

Level Designation	Data Product Description
Level 0	raw CCSDS payload and telemetry from space vehicles
Level 1a	Timestamped, geolocated, calibrated antenna temperature
Level 1b	Timestamped, geolocated, calibrated brightness temperature with bias removed
Level 2a URRP	Spatially resampled (i.e., collocated) brightness temperature (F-band resolution)
Level 2b	Atmospheric Vertical Temperature Profile [kelvins]
	Atmospheric Vertical Moisture Profile Profile [g/kg]
	Instantaneous Surface Rain Rate [mm/hr]
	TC Intensity: Minimum Sea-level pressure [mb]
	TC Intensity: Maximum Sustained Wind [m/s]

6 Retrieval Physics

This section reviews the atmospheric physics that the retrieval algorithm utilizes. For AVTP and AVMP, the primary mechanism is the radiative emission of atmospheric constituents. For microwave emission, the primary energy storage is rotational energy of the oxygen molecules for temperature and water vapor molecules for moisture. Figure 2 shows how the TROPICS F- and G-band channels are contiguous along the absorption line, which due to pressure line broadening, allows the channels to sound the atmosphere. The resulting temperature weighting functions are shown in Figure 4. Figure 3 has the passbands most sensitive to water vapor emission. The resulting water vapor burden, or the vertical sensitivity to water vapor density (kg/m^2), is shown in Figure 5.

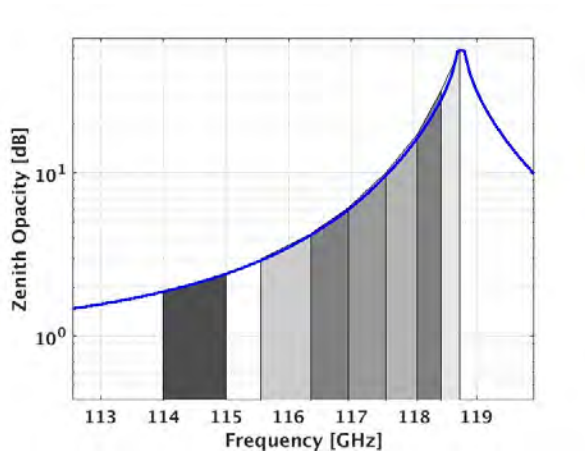

Figure 8 TROPICS passbands on the 118.76 GHz O2 absorption line.

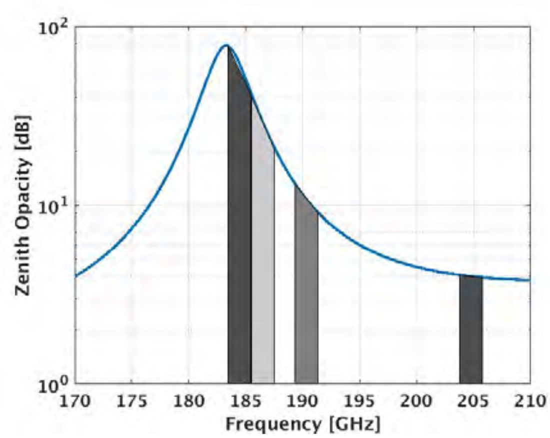

Figure 9 TROPICS passbands around the 183.31 GHz absorption line.

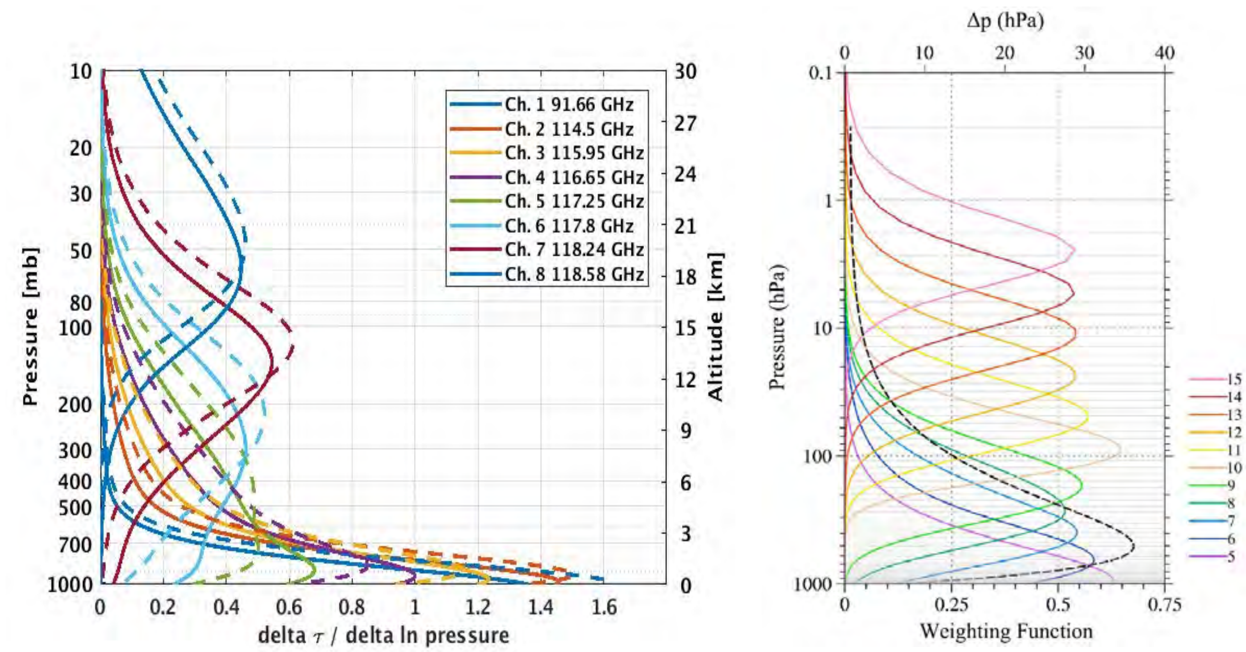

Figure 10 Left: Resulting TROPICS W- and F-band temperature weighting functions in a tropical standard 1976 atmosphere. The dashed lines are at 50 deg. incident angle, and the solid are nadir. Right: Weighting functions for the Advanced Technology Microwave Sounder (ATMS) temperature channels (5–15) are also shown for comparison (Tian and Zou 2016).

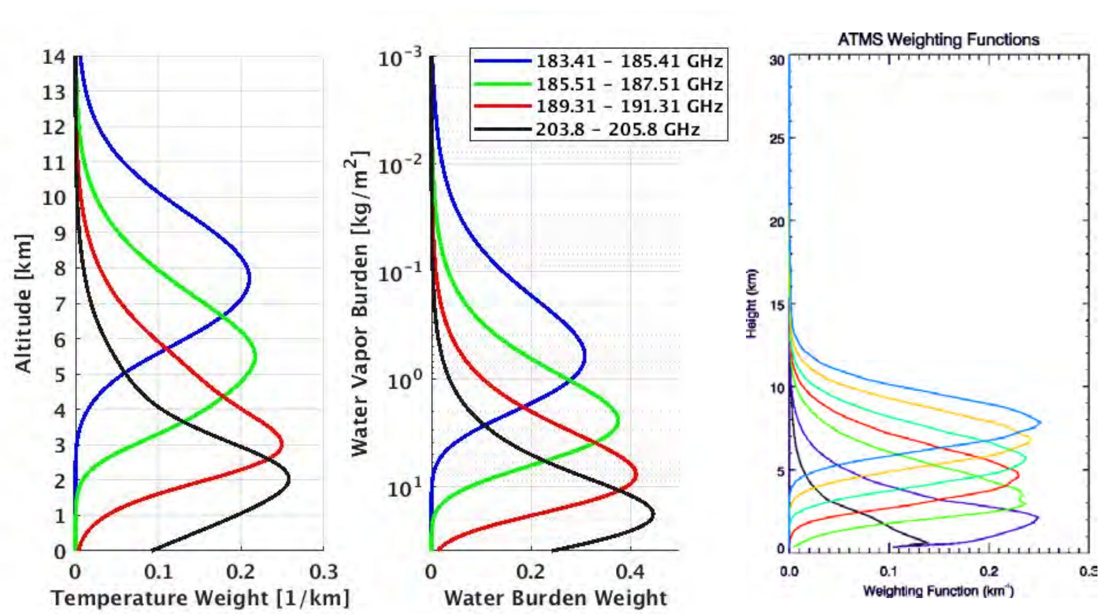

Figure 11 Left and middle: Resulting TROPICS G-band temperature and water vapor burden weighting functions in the tropical standard 1976 atmosphere. Right: Weighting functions for the ATMS moisture channels (16-22) are shown for comparison (Courtesy of S. Boukabara).

7 Algorithm Description

The TROPICS AVTP and AVMP will leverage existing algorithms that meet requirements, have been extensively tested and proven robust in operations, and save development cost. TROPICS has adapted the NOAA/NESDIS/STAR Microwave Integrated Retrieval System (MIRS) to the TROPICS payload.

The MIRS one-dimensional variational (1DVAR) approach to the retrieval problem is referred to as "advanced" as being more optimal compared to heritage algorithms and incorporates a sophisticated forward operator, which the heritage algorithms do not have, that fully assimilates all sensor radiance measurements (Boukabara et al. 2006). It is schematically represented in Figures 6 and 7 and mathematically seeks to minimize the following cost function (Boukabara et al. 2011; Boukabara et al. 2013):

$$J(X) = \left[\frac{1}{2}(X - X_0)^T B^{-1}(X - X_0)\right] + \left[\frac{1}{2}(Y^m - Y(X))^T E^{-1}(Y^m - Y(X))\right]$$

where X_0 and B are the mean background (i.e., a prior) and error covariance matrix of X, which is the state vector to be retrieved, respectively. Y^m and $Y(X)$ are the measurement vector and observation operator, respectively, and E is the measurement and/or modeling error covariance matrix.

The observation operator used by MIRS is the Community Radiative Transfer Model (CRTM) developed by the Joint Center for Satellite Data Assimilation (JCSDA). The CRTM produces the forward radiances $Y(X)$ as well as the Jacobians K (derivative of Y with respect to X). These are used in locating the minimum of $J(X)$ under the following condition:

$$\frac{\partial J(X)}{\partial X} = 0$$

and applying an iterative approach based on background departures (Boukabara et al. 2011):

$$\Delta X_{n+1} = [BK_n^T(K_n B K_n^T + E)^{-1}][(Y^m - Y(X_n)) + K_n \Delta X_n]$$

where n is the iteration index. At each iteration, the optimal departure from the background is updated given the derivatives as well as the covariance matrices. The iterations end when the following unconstrained cost function is used as a metric for deciding if convergence has been reached:

$$\chi^2 = [Y^m - Y(X)]^T E^{-1}[Y^m - Y(X)].$$

By default, convergence is achieved when $\chi^2 \leq 1$. The iterations may also end if the convergence criterion is not met within the default of 7 iterations (Zhang et al. 2014).

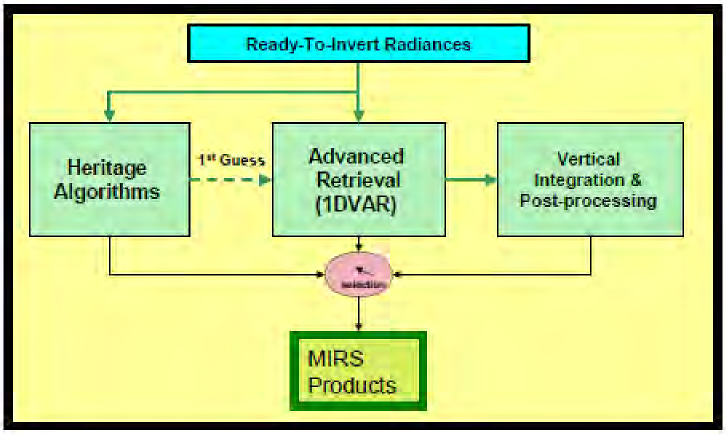

Figure 12 MIRS high-level conceptual diagram of the inversion processing block (Zhang et al. 2014).

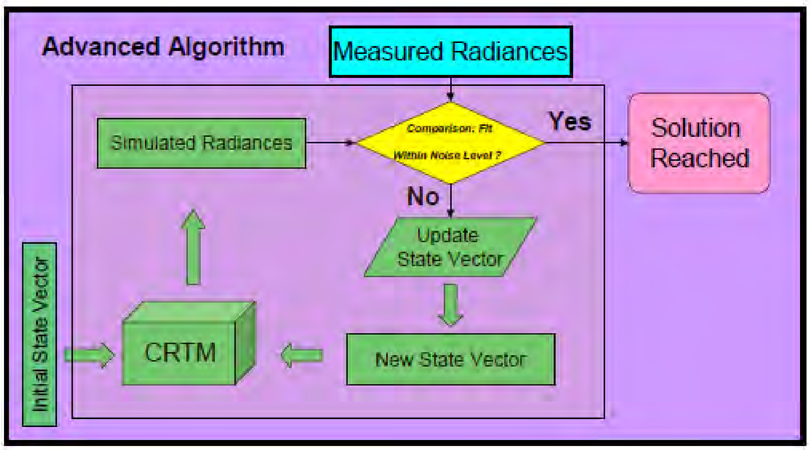

Figure 13 MIRS general description of the 1DVAR retrieval iterative system (Zhang et al. 2014).

7.1 Algorithm Input and Outputs

MIRS is driven by a master control file that allows a user to set a long list of parameters that control many aspects of the processing. These include the number of profiles to process, the number of retrieval attempts, whether external data are needed, geographic limits, among others. The file also allows the user to specify the names of the number of input files needed to run MIRS, which include information as to what atmosphere/surface Environmental Data Records (EDRs) are to be retrieved, bias corrections for the radiance measurements, covariance matrices for the background, forward radiative transfer model errors, and instrument noise specifications (Table 4). The EDRs that MIRS is able to retrieve are listed in Table 5. Note that all profiles are output as layers (as opposed to levels) since the CRTM requires layer absorber and cloud quantities. These 100 layers are bound by the same 101 pressure layers used in the production of Atmospheric Infrared Sounder (AIRS) single field-of-view temperature/moisture profile products (e.g., Strow et al. 2003). In addition, MIRS uses a global high-resolution surface elevation database from the United States Geological Survey that is used to assign a fixed surface pressure and surface type to the retrievals (personal communication, Chris Grassotti).

Table 4 MIRS input and output files used for TROPICS.

File name	Description
biasCorrec_tropics.dat	Bias adjustments to remove systematic differences between the forward operator and the actual measurements
TunParams_tropics.in	Select EDRs to retrieve, set number of EOFs and retrieval solution convergence parameters, etc.
CovBkgMatrxTotAtm_all.dat	Background covariance and transformation matrices for the atmospheric parameters based on 6-hourly 5° gridded climatology of ECMWF analyses for different seasons
CovBkgMatrxTotSfc_all_tropics.dat	Background covariance and transformation matrices for the surface EDRs as well as the background values
atmBkg_ECMWF_bin.dat	Binary file containing the atmospheric background values from ECMWF forecasts
ModelErrFile_tropics.dat	Assumed forward model errors
Tropics_NoiseFile_combo.dat	Noise specifications for instrument
Product swath binary file	Output binary file containing information pertaining to the inputs selected and the results of the retrievals, including the EDRs, quality control flags, and forward simulated radiances
Derived product swath binary file	Output binary file containing information derived from EDR parameters through vertical integration and post-processing algorithms

Table 5 Available EDRs for MIRS retrievals.

Parameter	Description
TEMP	Temperature vertical profile at 100 layers
WVAP	Water vapor mixing ratio vertical profile at 100 layers
CLW	Cloud liquid water mixing ratio vertical profile at 100 layers
RAIN	Rain mixing ratio vertical profile at 100 layers
SNOW	Snow mixing ratio vertical profile at 100 layers
ICE	Ice cloud mixing ratio vertical profile at 100 layers
GRPL	Graupel mixing ratio vertical profile at 100 layers
TSKIN	Surface skin temperature
EMIS	Surface emissivity
REFL	Surface reflectivity
WINDSP	Near-surface wind speed

The product swath binary output file contains important information related to the quality of the retrievals. These include a flag that describes the general validity of all the retrieved EDRs; i.e., whether they are "good," "use with caution," or "bad." The latter two rankings are determined by other information related to convergence of the solution, the presence and type of precipitation, out-of-bounds values, the detection of temperature lapse rate, temperature inversion, super saturation, humidity inversion and cloud detection. Also, other quality parameters include convergence metrics, i.e., χ^2 and the forward simulated radiances (Liu et al. 2016).

Because the MIRS code is modular and organized in a way that makes it relatively easy to add other sensors, modifications to the code needed to adapt MIRS to TROPICS were relatively minor. The most important and challenging modifications involved providing the proper input files. Perhaps the most difficult were the covariance and transformation background matrices needed for the surface parameters since these are sensor specific. To make these matrices consistent with those of the other MIRS-supported sensors, the MIRS team provided us with the necessary processing software (Fortran/IDL) needed to generate the background covariance and transformation matrices for TROPICS (personal communication, Shu-Yan Liu).

7.2 Algorithm Optimization

One way in which the 1DVAR algorithm in MIRS is optimized is the use of Empirical Orthogonal Function (EOF) decomposition for greater numerical stability and algorithm speed (Boukabara et al. 2011). The retrieval is done in reduced space by computing the EOFs for the geophysical background covariance matrix *B* in order to diagonalize it, i.e., construct a matrix that contains the eigenvalues and has eigenvectors that determine the new set of orthogonal axes. This transformation has the effect of improved handling of the strong correlations that can occur naturally between atmospheric parameters by significantly reducing oscillations. It also results in a savings in computational time because smaller matrices are used (Boukabara et al. 2011).

8 Forward Modelling

The TROPICS AVTP/AVMP algorithm requires two simulation systems. The algorithm uses the CRTM which has had coefficients for its fast atmospheric transmittance model and look-up (LUT) tables of cloud/precipitation single-scattering properties created specifically for the TROPICS payload and space vehicle platform. The second system consists of line-by-line model calculations (Rosenkranz 2003) used to generate the transmittance coefficients and state-of-the-art scattering calculations for ice particles (Ding et al. 2017) that were produced in conjunction with an instrument model. These calculations are performed in advance. However, the cloud/precipitation scattering LUT in the latest version of the CRTM has an upper limit of 190 GHz. Plans are to extend these tables to well beyond this limit to allow for more realistic scattering properties for the TROPICS 204.8 GHz channel.

For the upcoming Pathfinder mission, we have accounted for the polarization characteristics of TROPICS (i.e., polarization mixing occurs at a fixed zenith angle of about 20^o) in the CRTM, and used CRTM transmittance coefficients that have incorporated the measured spectral response functions (SRFs) of the instrument (for more details refer to the TROPICS Level-1 Radiance Algorithm

Theoretical Basis Document.) However, separate polarization mixing angles and CRTM spectral and transmittance coefficient files, will be needed for each of the six flight units in the constellation since they are expected to vary from instrument to instrument.

9 Algorithm Ancillary Data

The TROPICS AVTP/AVMP algorithm requires ancillary data in addition to the TROPICS space vehicle telemetry. These include the CRTM atmospheric transmittance model coefficients and LUTs of individual payload characteristics. The CRTM coefficients will be derived for each space vehicle based on the measured spectral response function and polarization.

10 Pre-launch Performance Testing

10.1 Data Description

The TROPICS AVTP/AVMP algorithm performance was verified pre-launch using the NOAA88 radiosonde dataset and European Centre for Medium-Range Weather Forecasts (ECMWF) model forecasts. While in situ measurements from radiosondes are important for verifying satellite retrievals, model data can provide far greater coverage and include cloud and precipitation properties. Studies have shown that the ECMWF temperature and water vapor forecasts agree well with in situ measurements (Dyroff et al. 2014), confirming that they provide sufficient realism for verifying the AVTP/AVMP products.

The source of the NOAA88 data is the National Environmental Satellite and Data Information Service (NESDIS) collocated radiosonde-satellite archive known as DSD5, whose main purpose is to investigate errors in radiosonde data and radiative transfer models (Uddstrom and McMillin 1994; Moncet et al. 2001). In this archive, the original radiosonde data (believed to have been collected at 14 mandatory levels under clear sky and cloudy conditions) were interpolated to the “TOVS 40” pressure levels (Weinreb et al. 1981). These 40-level profiles were further interpolated onto a 66-level standard grid with a minimum pressure of 1 hPa (Moncet et al. 2001). The 1988 subset of the global DSD5 dataset (i.e., NOAA88) consists of 8344 atmospheric profiles of pressure layer mean water vapor and pressure level temperatures, as well as surface pressure, skin temperature, latitude, longitude and date. Confining the tests to the oceans and ±40° latitude (the range of the TROPICS swath) provided a total of 714 profiles. Figures 8 and 9 show the locations and mean characteristics, respectively, of these profiles.

The ECMWF data were made available by the EUMETSAT Satellite Application Facility on Numerical Weather Prediction (NWP SAF; Erasmaa and McNally 2014). The entire NWP SAF database consists of 25,000 profiles (137 vertical levels) from global operational 36, 42, 48, and 54-hour forecasts starting at 00 UTC on the 1st, 10th and 20th days of each month for Sep 2013-Oct 2014. These profiles include temperature, water vapor, ozone, cloud ice water (CIW), cloud liquid water, rain rate and snow rate. We utilized 5 subsets of this database based on randomized sampling of the full database that provided a diversity of atmospheric conditions (Erasmaa and McNally 2014). We further reduced these data subsets according to whether they were clear-sky or cloudy. Model profiles classified as clear-sky were based on a threshold of combined vertically integrated CLW and CIW (liquid water path LWP and ice water path IWP) of less than 0.01 kg/m^2 (see Figures 10 and 11). To evaluate the performance of the AVTP/AVMP retrievals in cloudy conditions, profiles were selected that contained not only non-precipitating clouds ($LWP+IWP \geq 0.01\ kg/m^2$) but also lightly precipitating cases (vertically integrated rain rate of less than 0.2 mm/hr) (see Figures 12 and 13). Each hydrometeor profile was scaled by the maximum layer cloud cover to better represent these quantities over the model grid boxes.

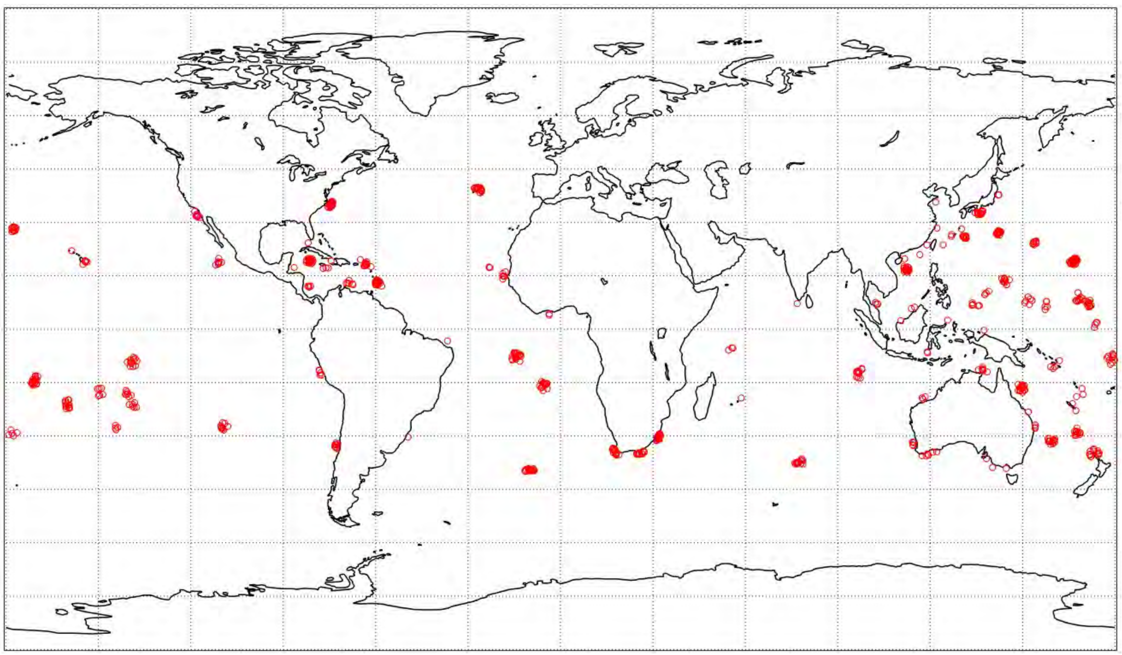

Figure 8 Locations of the NOAA88 profiles used in the performance testing.

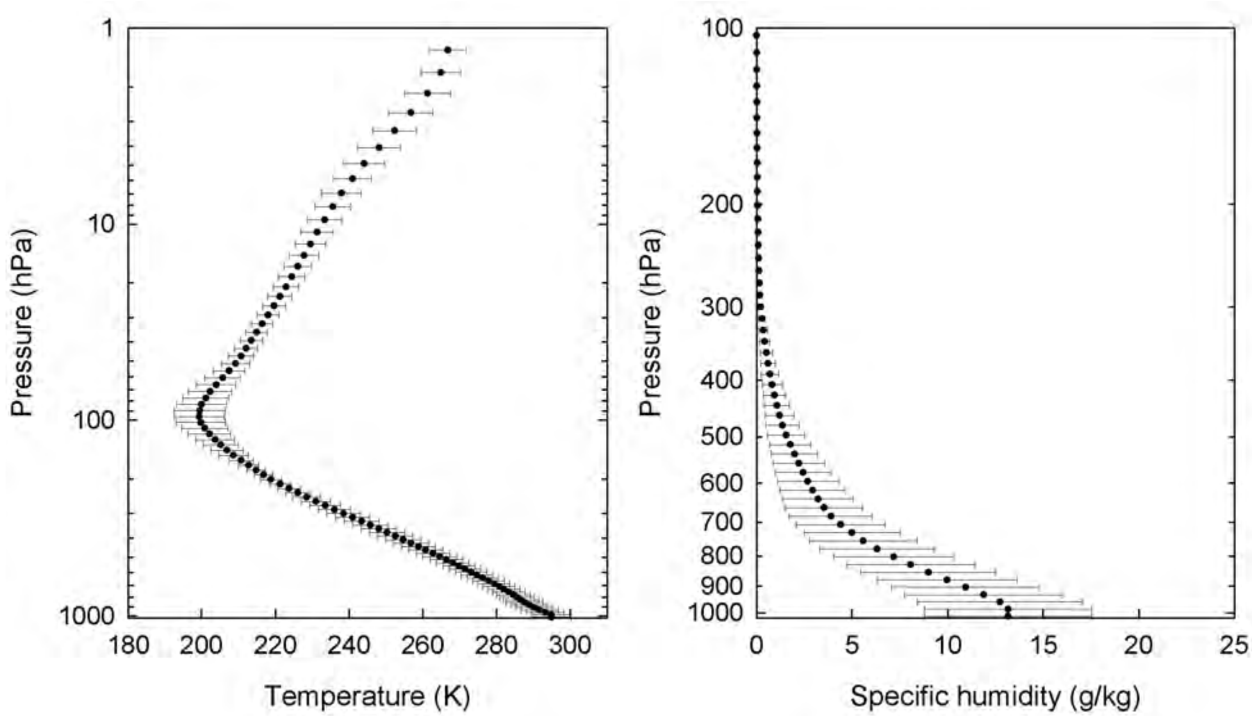

Figure 9 Characteristics of the NOAA88 profiles (interpolated to the MIRS 100 layers).

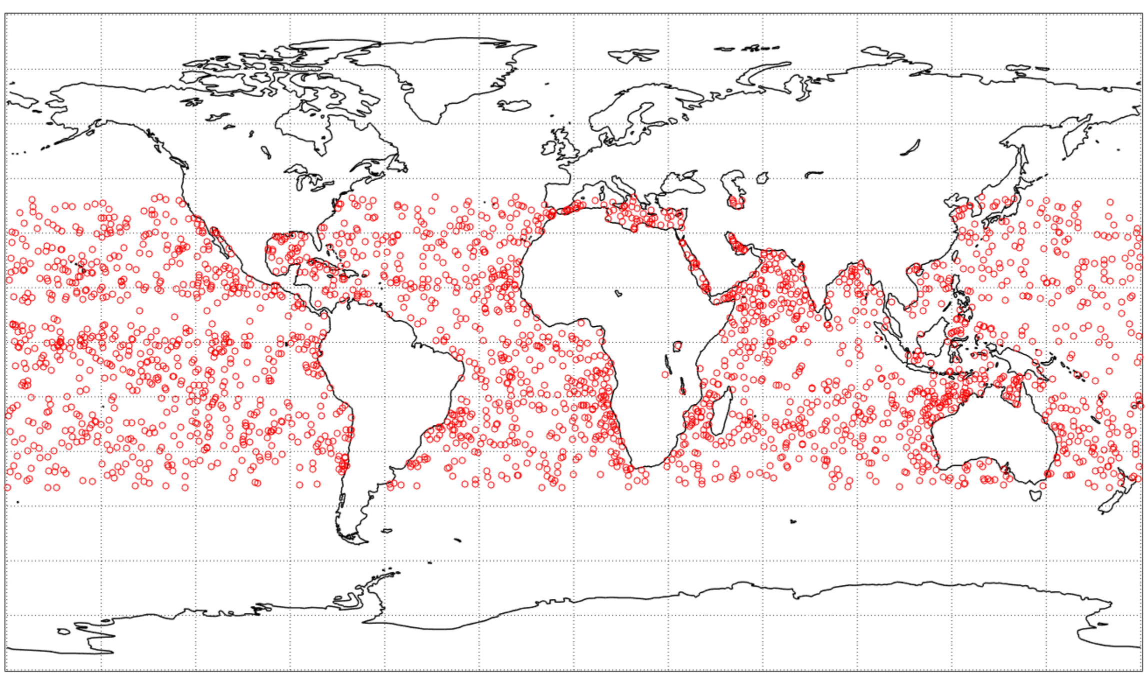

Figure 10 Locations of the NWP SAF clear sky profiles used in the performance testing.

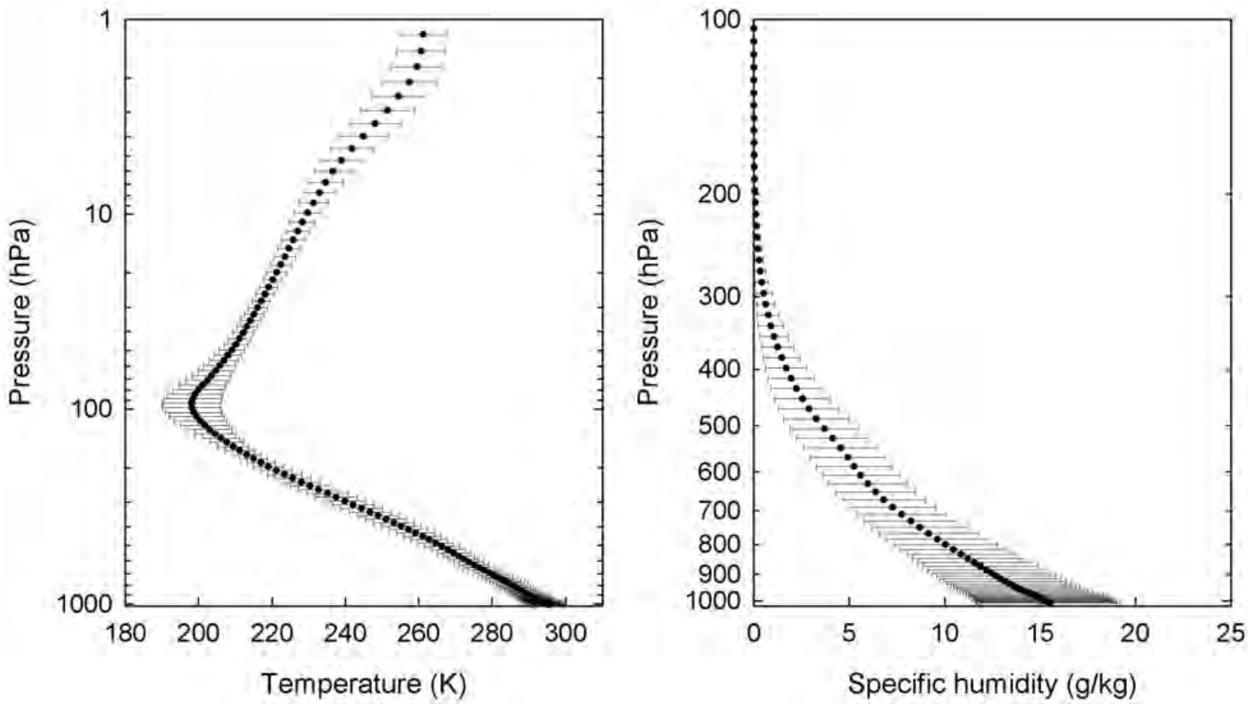

Figure 11 Characteristics of the NWP SAF clear sky profiles.

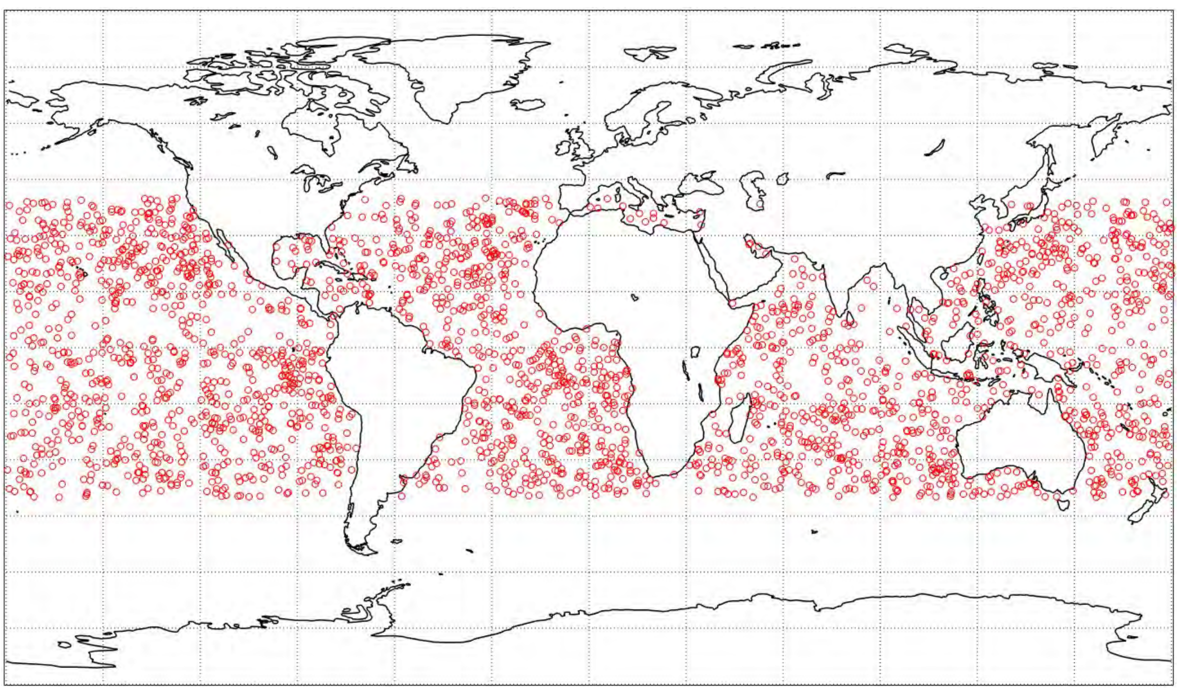

Figure 12 Locations of the NWP SAF cloudy profiles used in the performance testing.

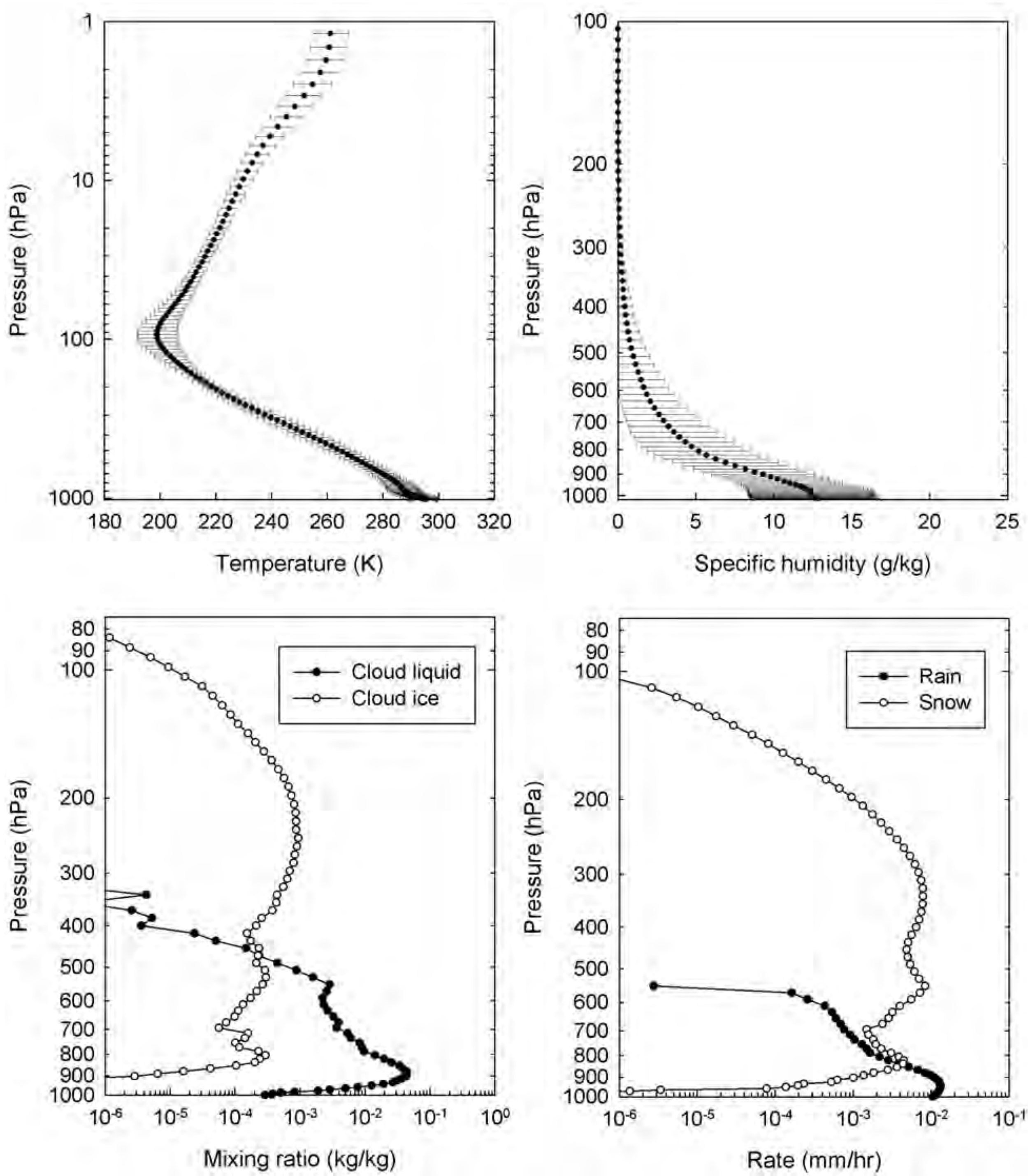

Figure 13 Characteristics of the NWP SAF cloudy profiles.

10.2 MIRS Configuration

The 1DVAR tuning parameters in the *TunParams_tropics.in* file were specified approximately to those used operationally for the Advanced Technology Microwave Sounder (ATMS). For example, the number of EOFs assumed in the retrievals of TEMP (i.e., AVTP), WVAP (i.e., AVMP), CLW, TSKIN and EMIS was based mainly on the ATMS but with three differences (see Table 6). Most of these changes were made based on a sensitivity analysis to slightly improve the performance of the AVMP retrievals. If the retrieval failed to converge, such as in the presence of precipitation, a second attempt was made that removes the CLW profile as an EDR and replaces it with the RAIN and GRPL profiles, which follows that used operationally for the ATMS (Table 6).

Other modifications were made to the instrument/forward model errors, which play an important role in the MIRS 1DVAR algorithm. The departure from the measured brightness temperatures is normalized by the instrument noise and forward model uncertainty. Depending on the signal-to-noise ratio, this normalization can determine which channels contain sufficient information in relation to the errors and which do not (Liu et al. 2016). Here, the instrument errors were assumed to be the NEdT values shown in Table 1, whereas the forward model errors were assumed to follow those used for the operational ATMS retrievals (specified in the *ModelErrFile_tropics.dat* and *NoiseFile_combo.dat* input files; see Table 7). An extensive sensitivity analysis revealed, however, that reducing these errors for the five TROPICS moisture channels had the largest impact on significantly improving the performance of the AVMP retrievals. As a result, errors were scaled by 0.5 in the tuning parameters input file for only these channels in order to maximize performance.

The iterative solution for the 1DVAR algorithm requires a first guess and a constraint. In our analysis we used the default settings for MIRS, which is a climatology as the background (see Table 4) that also serves as the first guess.

Table 6 Number of EOFs assumed in the TROPICS tuning parameter files. ATMS values are given in parentheses.

EDR	#EOFs (1st pass)	#EOFs (2nd pass)
TEMP	8	7
WVAP	6 (4)	5
CLW	3	0
RAIN	0	3
GRPL	0	3
TSKIN	1	0
EMIS	3 (4)	3 (4)

10.3 Analysis Method

To make use of the NOAA88 and NWPSAF datasets in the performance testing, we first generated synthetic TROPICS brightness temperatures (BTs) for these datatsets based on the same version of the CRTM used in MIRS for its forward calculations. In these calculations we did not consider the unusual polarization characteristics of the TROPICS instrument. Instead, for simplicity, we assumed the radiances were unpolarized (i.e., the first Stokes parameter) in the CRTM, which makes use of the average of the vertically and horizontally polarized surface reflectances in the forward calculations. Finally, instrument noise was added to the simulated BTs using the NEdT values from Table 1 with an assumed Gaussian noise distribution.

Table 7 Forward model and instrument errors assumed in the MIRS retrievals.

Chan.	Center Freq. (GHz)	Forward model error (K)	NEdT (K)
1	91.655 ± 1.4	1.445	0.60
2	114.50	0.550	1.00
3	115.95	0.600	0.90
4	116.65	0.700	0.90
5	117.25	0.700	0.90
6	117.80	0.750	0.90
7	118.24	0.850	0.90
8	118.58	1.000	1.00
9	184.41	1.020	0.60
10	186.51	0.984	0.60
11	190.31	1.116	0.60
12	204.8	1.083	0.60

The process of directly comparing the MIRS temperature/moisture profile retrievals to the NOAA88 and NWPSAF profiles was accomplished in two steps. First, when comparing observed retrievals to other observations or model data with higher vertical resolution and with much less dependence on their a priori information, it is appropriate to prepare a higher resolution profile (X_h) for comparison to a lower vertical resolution retrieval (i.e., from MIRS) by linearly weighting X_h and the background profile used in the retrieval (X_0) as (Rodgers and Connor 2003):

$$X_s = X_0 + A(X_h - X_0) \quad (1)$$

where X_s is the “smoothed” profile and the averaging kernel matrix A, which may be interpreted as a measure of the contributions of the measurements relative to the background in the retrieval, is defined as:

$$A = GK$$

and where G is the "gain" or "contribution" matrix

$$G = BK^T(KBK^T + E)^{-1}$$

One caveat of this approach is that if A=0 (i.e., the measurements contain no information), all of the information will originate from the background assumed in the retrievals, in which case the error between the retrieval and the "truth" profile will be exactly zero when in fact the measurements contain no information. With respect to the TROPICS instrument, however, this is only likely to occur at higher altitudes that are beyond the sensitivity of the TROPICS channels.

Since we use the logarithm of the water vapor mixing ratio as a state variable in MIRS (users can select either linear or logarithm), eq. (1) should be expressed as follows when comparing moisture profiles:

$$\log(X_s) = \log(X_0) + A \log(X_h/X_0)$$

Figure 14 illustrates the results of applying the kernel smoothing to a sample NWP SAF profile. It is worth noting that the operational version of the MIRS code does not actually output the A matrix even though it does contain the subroutines to compute this matrix. We used these subroutines along with designating an additional value to the *RetrErrCharac* flag (i.e., output retrieval error characteristics) inside the tuning parameters input file as a way for users to output the A matrix.

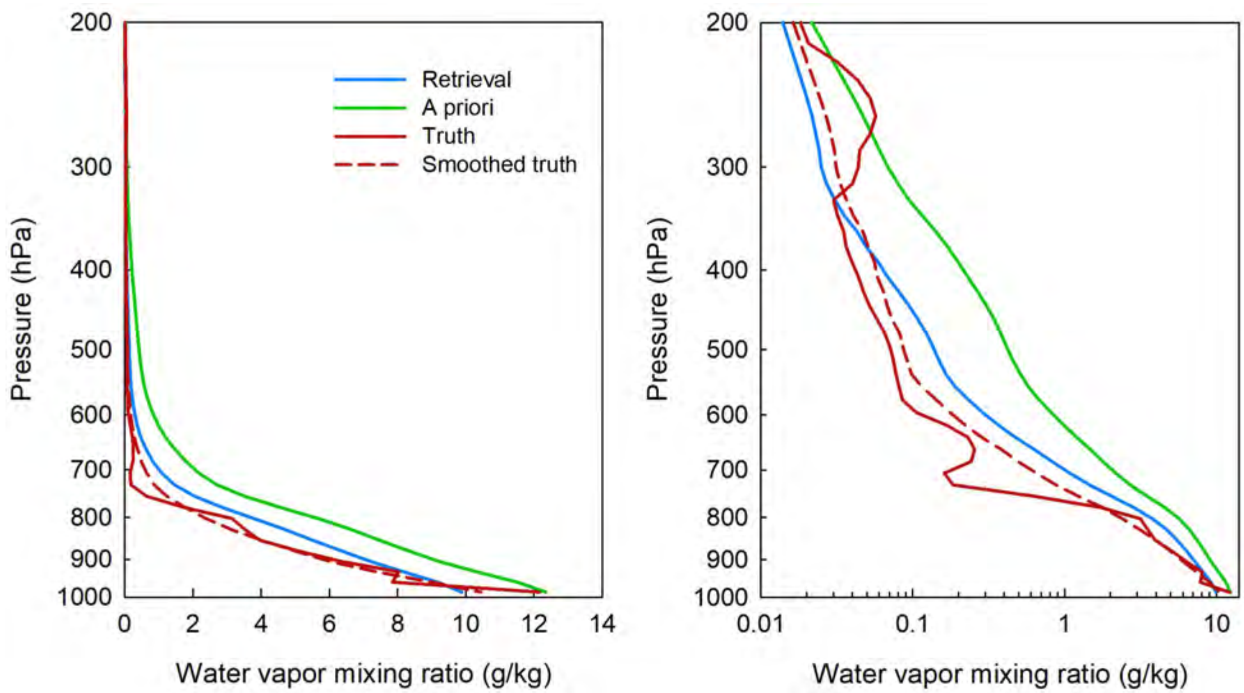

Figure 14 A smoothing example using the averaging kernel (shown on both linear and log scales), where "truth" is a NWP SAF clear sky profile and "a priori" is the climatology background used in the retrieval.

Once the averaging kernels have been applied to the NOAA88 and NWP SAF profiles, the remaining step is to compute the root-mean-square deviation (RMSD) over coarse layers, which is the measure that has been selected by the TROPICS mission to quantify the performance of the MIRS retrievals relative to the two reference datasets. The first step in the procedure is to compute the mean temperature and water vapor mixing ratio values over 3-km layers for each profile. Seven coarse layers (0-3, 3-6, 6-9, 9-12, 12-15, 15-18, 18-21 km) are used for temperature and four coarse layers (0-3, 3-6, 6-9, 9-12 km) are used for water vapor. Then, the squared differences of the retrieval and reference values are summed over the number of profiles. In addition, the RMSD for water vapor mixing ratio is scaled by the mean mixing ratio in each coarse layer to represent it as a percentage.

10.4 Results

The performance of the MIRS AVTP/AVMP retrievals for the NOAA88 and NWP SAF clear sky datasets is shown as a function of height in Figure 15 under nadir conditions. Unless otherwise noted, all retrievals regardless of their quality were retained in the analysis. Details concerning the MIRS retrieval statistics, including quality control, are given in Table A1 of the Appendix.

Results indicate that the AVTP retrievals easily meet the baseline requirement of 2.0 K at all layers and for both datasets (see Table 8 for vertical means). The biases are also quite small. However, the AVMP retrievals do not perform quite as well and exhibit relatively larger biases but still meet the baseline requirement of 25% in the lowest 9 km for the NOAA88 dataset and when averaged over all coarse layers for both datasets (Table 8). Why the performance of the MIRS AVMP is poorer for the NWP SAF dataset is not clear. It may be a result of the different profile characteristics, such as larger variations in mid-tropospheric water vapor than in the NOAA88 dataset. A cursory examination of Figures 9 and 11 seems to suggest this.

Another comparison can be made with the ATMS, which represents the standard in passive microwave retrievals of temperature and water vapor profiles. The same analysis methods used for the TROPICS retrievals were also applied to the ATMS retrievals; however, because MIRS uses bias corrections for the ATMS, these values were removed from the input bias correction file for this exercise. It is not entirely unexpected that the TROPICS AVTP retrievals do not perform nearly as well as the ATMS retrievals (see Figure 15), where the vertical mean RMSDs are larger by 0.40-0.47 K for both datasets (Table 8). However, it is somewhat surprising that the vertical means of the RMSD for the AVMP retrievals differ by only 1.7-1.8% and suffer from similar biases (Table 8 and Figure 15). But if one compares only those retrievals classified as "good" by the quality control flag, the differences increase to 2.3-4.3% (Table 8). This suggests that the ATMS retrievals classified as "use with caution" have significantly larger errors than similar TROPICS retrievals because the number of "good" retrievals relative to "use with caution" retrievals is about the same for both (Table A1).

Another useful metric to gauge the quality of the MIRS retrievals is to investigate the first moment of the vertical profile, that is the vertically integrated water vapor or total precipitable water (TPW). Results show that while the TROPICS TPW values are reasonably accurate, they exhibit greater variability and have larger TPW-dependent biases than the ATMS results (Figure 16). Simulations demonstrate this is caused primarily by the TROPICS sensor not having a low frequency water vapor channel (23.8 GHz) like the ATMS, which has greater sensitivity to TPW in moderately to very moist environments than the TROPICS 91.6 GHz channel.

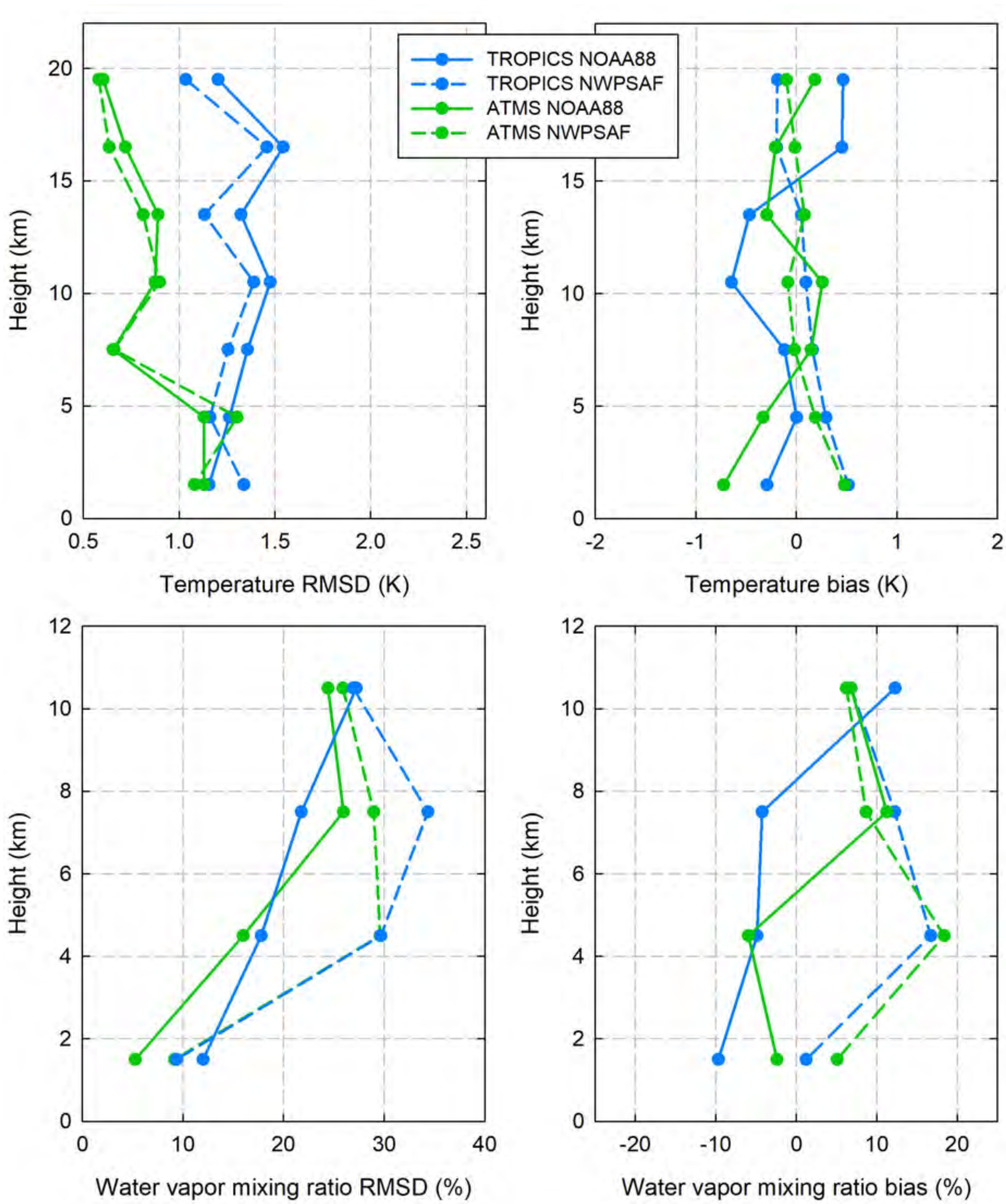

Figure 15 Error characteristics of the TROPICS (blue) and ATMS (yellow) retrievals for the NOAA88 and NWP SAF clear-sky profiles at nadir.

Table 8 Summary of vertically-averaged performance results for TROPICS and ATMS.

TROPICS				
	All retrievals		"Good" retrievals only	
Dataset	AVTP RMSD (K)	AVMP RMSD (%)	AVTP RMSD (K)	AVMP RMSD (%)
NOAA88	1.33	19.7	1.26	19.3
NWPSAF clear-sky	1.25	25.1	1.24	23.9
NWPSAF cloudy	1.23	24.3	1.21	22.5
ATMS				
	All retrievals		"Good" retrievals only	
Dataset	AVTP RMSD (K)	AVMP RMSD (%)	AVTP RMSD (K)	AVMP RMSD (%)
NOAA88	0.86	17.9	0.74	15.0
NWPSAF clear-sky	0.85	23.4	0.82	21.1
NWPSAF cloudy	0.83	21.8	0.79	20.2

In cloudy conditions, results show that the MIRS AVTP retrievals perform nearly the same vertically and in terms of vertically-averaged RMSD as the clear-sky cases (Figure 17 and Table 8). Similar results are seen in the AVMP retrievals, although the vertical mean RMSD is slightly better than the clear-sky cases (the ATMS retrievals also behave in the same way). This may seem contradictory but is likely related to the vertical characteristics of the water vapor profiles being somewhat different between the clear-sky and cloudy cases (cf. Figures 11 and 13). In any case, these differences are not deemed to be statistically significant. It is important to emphasize these error estimates are not expected to represent all retrievals in cloudy conditions since tropical cyclones, for example, often contain thick clouds with heavy precipitation, which will greatly degrade the quality of the AVTP/AVMP retrievals.

Another consideration is how the performance of the TROPICS retrievals changes with respect to varying zenith angle. Results show that the RMSD decreases nonlinearly with increasing zenith angle (Figure 18) for both temperature and moisture. The reductions in RMSD between nadir and the edge of the scan are 0.13 K and 2% for the AVTP and AVMP retrievals, respectively.

The impact of changing instrument noise levels on the AVTP/AVMP retrievals should also be examined because they can change over the lifetime of the instrument. To investigate this effect, we simply added noise with a standard deviation of 0.5 K to all TROPICS channels with nominal NEdT values indicated in Table 1 by taking the root sum squared of the two quantities for each channel. The analysis shows that the AVTP retrievals are largely unaffected by the increased noise levels, with increased RMSDs of less than 1 K, regardless of the dataset or whether all or only "good" retrievals are included (Table 9). On the other hand, the RMSDs for the AVMP retrievals increased by about 2% for all datasets and, when including all retrievals, caused the RMSDs to slightly exceed the baseline requirement of 25% for the NWP SAF clear sky and cloudy datasets. When considering only "good" retrievals the increase in RMSD was slightly less pronounced (0.6-1.8%).

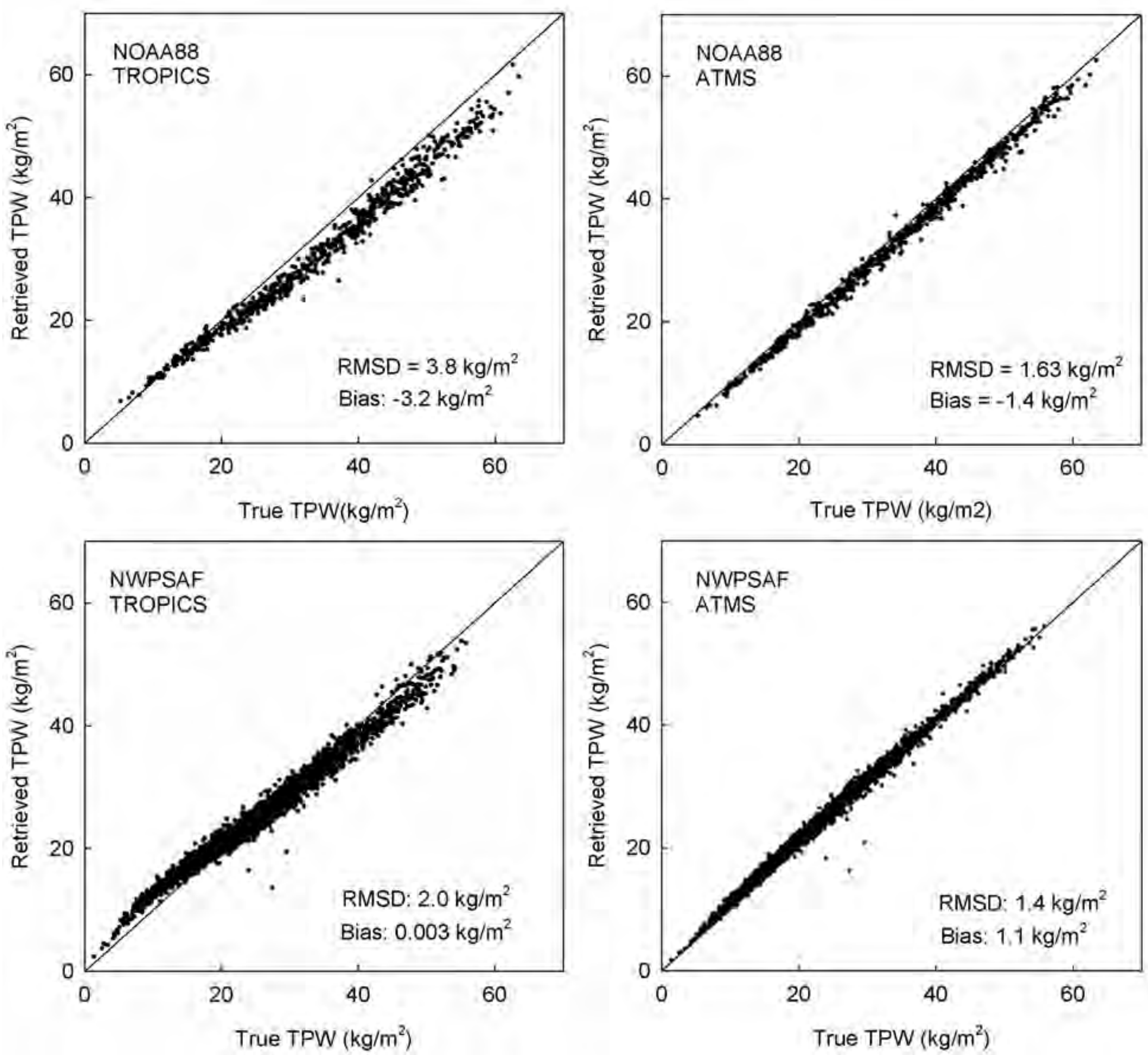

Figure 16 Total precipitable water (TPW) from TROPICS and ATMS retrievals for NOAA88 and NWP SAF clear-sky profiles.

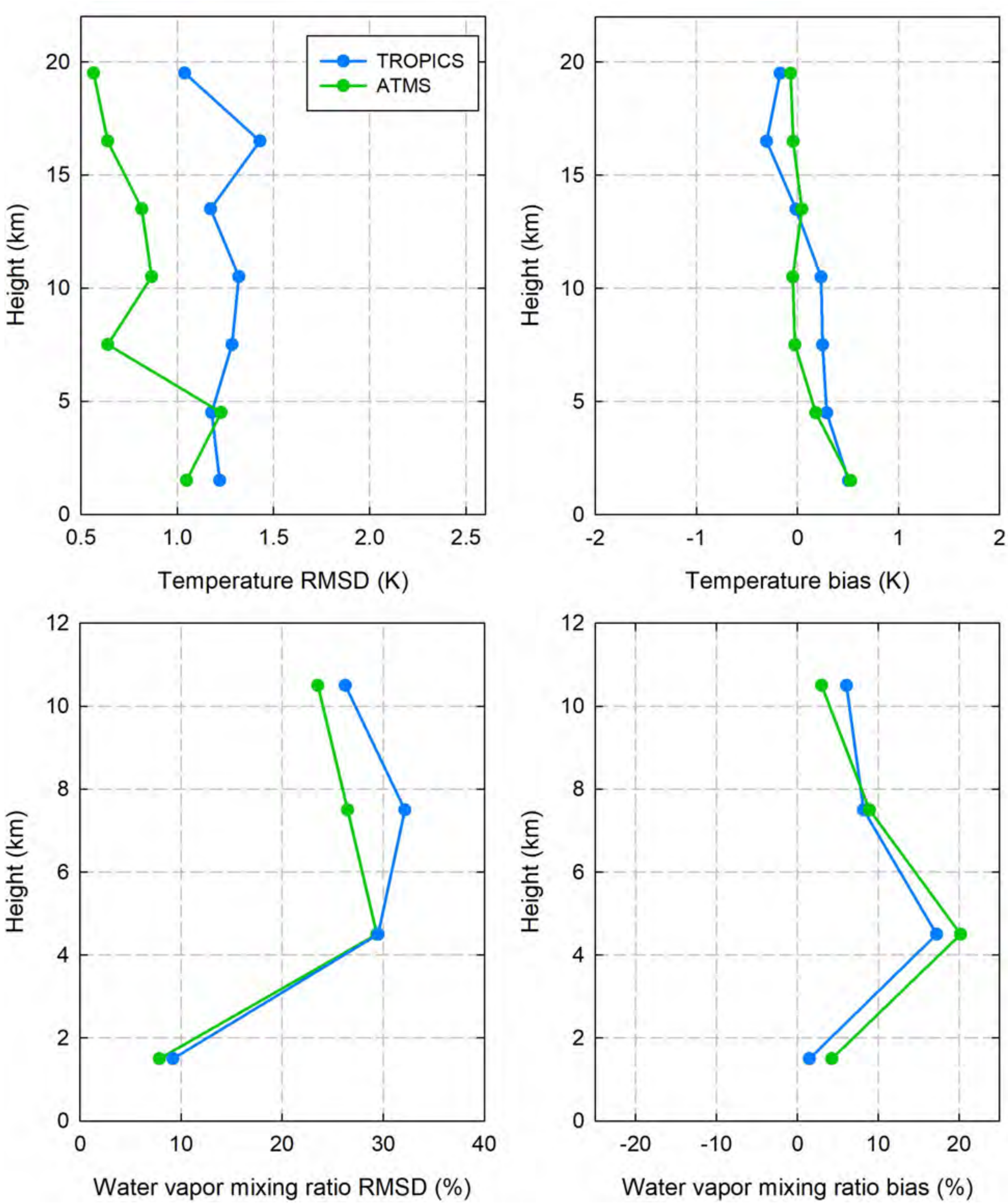

Figure 17 Error characteristics of the TROPICS and ATMS retrievals for NWP SAF cloudy profiles at nadir.

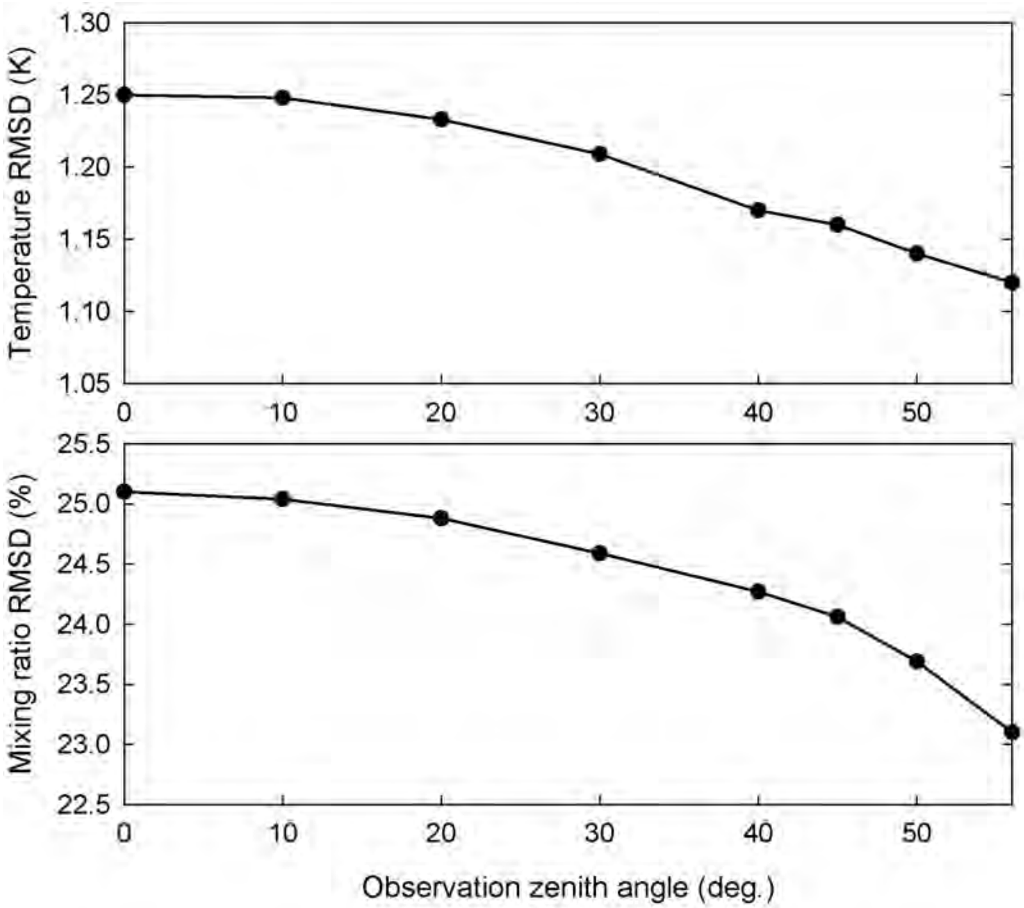

Figure 18 Variation of the RMSDs with observation zenith angle for the NWP SAF clear-sky dataset.

Table 9 Summary of vertically-averaged performance results for TROPICS assuming an increase in instrument noise.

	All retrievals		"Good" retrievals only	
Dataset	AVTP RMSD (K)	AVMP RMSD (%)	AVTP RMSD (K)	AVMP RMSD (%)
NOAA88	1.40	20.9	1.34	19.9
NWPSAF clear-sky	1.33	27.3	1.31	25.7
NWPSAF cloudy	1.32	26.3	1.29	24.1

10.5 Application with Real TROPICS Data

The operational MIRS is currently set up to use climatology as the background and first guess in the 1DVAR algorithm. However, in practice, we will improve the performance of the TROPICS AVMP products by exploiting forecast model data. In the tuning parameters control file, MIRS provides a flexible means of assigning which external datasets are used for each state variable through a control parameter. Via this option, it is possible to use forecast model data as background and first guess external data for MIRS. For both the Pathfinder and Constellation missions, we will use Near-Real Time (NRT) Goddard Earth Observing System 5 (GEOS-5) forecast products from the NASA Global Modeling and Assimilation Office (https://gmao.gsfc.nasa.gov/GMAO_products/NRT_products.php).

Unlike the simulations, however, we will need to derive a set of bias corrections (see Table 4) when using actual TROPICS data. We will accomplish this by computing the difference between the observations and the forecast background (i.e., O-B) for clear sky scenes over a sufficient time. These bias corrections will vary according to channel and scan angle.

Another benefit of using forecast model data is to replace the current practice in MIRS of setting the surface pressure in the retrievals to a fixed value of 1008 hPa over the oceans. Having a more accurate surface pressure over ocean and land surfaces will help to mitigate the problems that can occur near the center of cyclonic weather systems where the surface pressure can be significantly smaller than that assumed in the retrievals. The result is that retrievals occurring at pressure layers below the pressure level at the surface will be effectively underground. We will consider implementing this improvement in a future version of the TROPICS AVMP products.

11 Appendix

Table A1 MIRS retrieval statistics for the TROPICS and ATMS.

TROPICS						
Dataset	Total profiles	Convergence rate (%)	Mean iterations per profile	“Good” retrievals	Use with caution	“Bad” retrievals
NOAA88	714	98.4	2.1	417	297	0
SAF clear-sky	2392	99.9	2.1	1734	658	0
SAF cloudy	2453	100	2.1	1758	695	0
ATMS						
Dataset	Total profiles	Convergence rate (%)	Mean iterations per profile	“Good” retrievals	Use with caution	“Bad” retrievals

NOAA88	714	99.7	2.0	360	354	0
SAF clear-sky	2392	99.9	2.1	1439	953	0
SAF cloudy	2453	100	2.0	1407	1046	0

12 References

Boukabara, S. A. , F. Weng , R. Ferraro , L. Zhao , Q. Liu , B. Yan , A. Li , W. Chen , N. Sun , H. Meng , T. Kleespies , C. Kongoli , Y. Han , P. Van Delst , J. Zhao and C. Dean, 2006: Introducing NOAA's Microwave Integrated Retrieval System (MIRS). Presentation at the ITSC-15 conference in Maratea, Italy.

Boukabara, S, K. Garrett, C. Grassotti, F. Iturbide-Sanchez, W. Chen, Z. Jiang, S. A. Clough, X. Zhan, P. Liang, Q. Liu, T. Islam, V. Zubko, and A. Mims, 2013: A physical approach for a simultaneous retrieval of sounding, surface, hydrometeor, and cryospheric parameters from SNPP/ATMS. *J Geophys. Res. Atmos.*, *118*, DOI: 10.1002/2013JD020448.2158438.

Boukabara, S, K. Garrett, W. Chen, F. Iturbide-Sanchez, C. Grassotti, C. Kongoli, R. Chen, Q. Liu, B. Yan, F. Weng, R. Ferraro, T. Kleespies, and H. Meng, 2011: MiRS: An all-weather satellite data assimilation and retrieval system. *IEEE Trans. Geosc. Rem. Sens.*, DOI: 10.1109/TGRS.2011.2158438.

Ding, J., L. Bi, P. Yang, G. Kattawar, F. Weng, Q. Liu, T. Greenwald, 2017: Single scattering properties of ice particles in the microwave regime: Temperature effect on the ice refractive index with implications in remote sensing. *J. Quant. Spect. Rad. Trans*., 190, 26-37.

Dyroff, C., A. Zahn, E. Christner, R. Forbes, A. M. Tompkins, and P. F. J. can Velthoven, 2015: Comparison of ECMWF analysis and forecast humidity data with CARIBIC upper troposphere and lower stratosphere observations, Quart. J. Royal Meteor. Soc., 141, 833-844.

Eresmaa, R., and A. P. McNally, 2014: Diverse profile datasets from the ECMWF 137-level short-range forecasts. NWP SAF Report No. NWPSAF_EC_TR_017, 12 p.

Liu, Q., C. Grassotti, K. Garrett, S. Liu, and S. Boukabara, 2016: NOAA/JCSDA Microwave Integrated Retrieval System (MIRS) User Manual, NOAA, NESDIS, STAR.

Moncet, J. L., S.-A. Boukabara, A. Lipton, J. Galantowicz, H. R.-Isaacs, J. Hegarty, X. Liu, R. Lynch, and N. Snell, 2001: Algorithm Theoretical Basis Document for the Conical-Scanning Microwave Imager/Sounder (CMIS) Environmental Data Records, Volume 2: Core Physical Inversion Module, Atmospheric and Environmental Research, Inc., Lexington, MA.

Rodgers, C. D., and B. J. Connor, 2003: Intercomparison of remote sensing instruments. J. Geophys. Res, 108, D3, doi:10.1029/2002JD002299.

Rosenkranz, P. W., 2003: Rapid radiative transfer model for AMSU/HSB channels. IEEE Trans. Geosc. Rem. Sens., 41, No. 2, 362-368.

Strow, L., L., S. E. Hannon, S. De Souza-Machado, H. E. Motteler, and D. Tobin, 2013: An overview of the AIRS radiative transfer model, IEEE Trans. Geosc. and Rem. Sens., 41, No. 2.

Tian, X., and X. Zou, 2016: ATMS- and AMSU-A-derived hurricane warm core structures using a modified retrieval algorithm, J. Geophys. Res. Atmos., 121, 12,630–12,646, doi:10.1002/2016JD025042.

Uddstrom, M. J., and L. M. McMillin, 1994: System noise in the NESDIS TOVS forward model. Part I: Specifications, J. Appl. Meteor., 33, 919-938.

Weinreb, M. P., H. E. Fleming, L. M. McMillin, and A. C. Neuen- dorffer, 1981: Transmittances for the TIROS operational vertical sounder. NOAA Tech. Rep. NESS, 85, 60 pp.

Zhang, X., C. Grassotti, K. Garrett, T. Islam, 2014: Microwave Integrated Retrieval System (MIRS) System Description Document. NOAA, NESDIS, STAR.